IEEE Access
Multidisciplinary | Rapid Review | Open Access Journal

Received December 20, 2019, accepted January 25, 2020, date of publication February 3, 2020, date of current version February 11, 2020.

Digital Object Identifier 10.1109/ACCESS.2020.2971003

Performance Enhancement of Robust Cubature Kalman Filter for GNSS/INS Based on Gaussian Process Quadrature

BINGBO CUI[1], (Member, IEEE), XINHUA WEI[1], XIYUAN CHEN[2], (Senior Member, IEEE), AND AICHEN WANG[1]

[1]Key Laboratory of Modern Agricultural and Technology, Ministry of Education and Jiangsu Province, Jiangsu University, Zhenjiang 212013, China
[2]Key Laboratory of Micro-Inertial Instrument and Advanced Navigation Technology Ministry of Education, School of Instrument Science and Engineering, Southeast University, Nanjing 210096, China

Corresponding authors: Bingbo Cui (cuibingbo@ujs.edu.cn) and Xinhua Wei (wei_xh@126.com)

This work was supported in part by the National Natural Science Foundation of China under Grant 31901416, in part by the Natural Science Foundation of Jiangsu Province under Grant BK20180859, in part by the China Postdoctoral Science Foundation under Grant 2019M651745, and in part by the Priority Academic Program Development of Jiangsu Higher Education Institutions under Grant PAPD-2018-87.

ABSTRACT The sigma-point Kalman filters are generally considered to outperform extended Kalman filter in the application of GNSS/INS, where cubature Kalman filter (CKF) is widely approved because of its rigorous mathematic derivation. In order to improve the robustness of GNSS/INS under GNSS-challenged environment, a robust CKF (RCKF) is developed based on novel sigma-point update framework (NSUF) in our previous work, whereas the efficiency of NSUF is still plagued by the unknown process model uncertainty. In this paper, an enhanced RCKF is proposed based on Gaussian process quadrature (GPQ), where the uncertainty consisted in sigma points transform is processed by GPQ conditioning on the approximated posterior PDF. Experiment result on loosely coupled GNSS/INS demonstrates the superiority of proposed method, where the heading error and roll error are reduced by 60.5% and 37.5% respectively compared with RCKF, and it achieves better position result than GP-CKF under GNSS outage.

INDEX TERMS Land vehicle navigation, sigma-point Kalman filter, Gaussian process quadrature, sigma points transform.

I. INTRODUCTION

Global navigation satellite system (GNSS) has been widely approved as an efficient tool for the navigation of land vehicle because of its superiority in all-weather condition and long-term high accuracy. However, GNSS suffers from frequently blocking and disturbances in the application of self-driving vehicle, making it be integrated with other navigation systems often rather than be used as a standalone system. Due to the complementary error properties of GNSS and inertial navigation system (INS), the integration of the two is a typical solution for seamless land vehicle navigation, where Kalman filter (KF) and its variants dominate the information fusion algorithms. For the filtering problem of linear state-model and be given precise prior knowledge, KF is the optimal solution in the minimum mean squared error (MMSE) under Gaussian hypothesis of underlying state. However, these conditions are hardly satisfied in real-world, where the time-varying uncertainty, large prior error and unknown noise properties are the most active research aspects of nonlinear filtering.

The error propagation model of INS is usually taken as the system model of GNSS/INS, where the nonlinearity resulting from large attitude error or position error cannot be neglected. To solve the nonlinearity problem contained in state estimation, many sub-optimal KF have been proposed, where extended Kalman filter (EKF) and unscented Kalman filter (UKF) are two famous solutions in navigation and target tracking application [1], [2]. Unlike EKF which linearizes the nonlinear model directly based on Taylor series expansion, UKF utilizes sigma points transform to match the moments of transformed random variable, which achieves better accuracy

The associate editor coordinating the review of this manuscript and approving it for publication was Shuai Han.

and is more easily to be implemented than EKF because of its derivative free merit. However, in the application of UKF, the filtering performance depends on the selection of scale parameters of sigma points generation [3]. What is more, it is reported that UKF becomes unstable with the increase of state dimension, and cubature Kalman filter (CKF) is more suitable for high-dimensional filtering problem [4]. From the number-integration perspective, many nonlinear filters are developed, such as high degree CKF [5] and sparse-grid quadrature filter [6], which however inherit the weakness of KF framework, i.e., problems of model uncertainty and unknown prior information. In order to enhance the robustness of KF, maximum correntropy criterion rather than the MMSE is used to update the posterior PDF under non-Gaussian noise [7], whose efficiency however, depends on the kernel parameters heavily. In order to handle the uncertainty contained in the process model of GNSS/INS, the M-estimation-based KF is developed [8], which is less efficient when uncertainties co-exist in the measurement and process model.

By stochastically approximating the posterior probability density function (PDF), particle filtering (PF) can handle the nonlinear and non-Gaussian filtering problem efficiently at the cost of prohibitive complexities [9]. Many extensions of PF have been proposed to reduce its complexity [10]–[12], which may still have problems in resampling or choice of importance function. What is more, it has been reported that the deterministic nonlinearity of GNSS/INS is mild, and the stochastic or uncertainty-induced nonlinearity is the main problem of filter divergence [13]. Recently, adaptive KFs based on variational Bayesian (VB) become conspicuous [14]–[16], because it can not only handle parameter identification and state estimation but also is efficient for high-dimensional state model estimation. In order to process the skew-t distributed noise, an improved skew-t filter is proposed by using VB [17]. However, it is hard to estimate the parameters of skew-t distribution due to the changes of sensor environment, and the Student's t filter may encounter new problems by using fixed scale matrix [18].

In the context of integrated navigation, the VB is often used to estimate the unknown parameters or time-varying measurement noise [19]. Recently, many works apply VB to the estimation of process noise covariance, e.g., an adaptive EKF is developed by identifying process noise and measurement noise online in [20]. However, it has been well recognized that the process noise cannot be estimated accurately based on limited observations of short duration. What is more, there is often state-dependent noise in GNSS/INS making the VB-based process noise estimation failed. In our previous work, the robustness of CKF under GNSS-challenged environment is enhanced by developing novel sigma-point update framework (NSUF), where the sigma points residues generated by the model prediction are transformed directly to construct posterior sigma points by considering the measurement uncertainty [21]. In order to process the time-varying measurement noise appeared in NSUF for GNSS/INS, a robust filter named as VB-RCKF is proposed in [22] by employing the VB to update the noise covariance. In order to fully utilize the emerged observation during a long GNSS outage, a combined NSUF is developed to handle the frequently appeared signal blocking that easily encounter in urban area [23]. Although VB-RCKF outperforms VB-CKF in terms of convergence and accuracy, it still suffers from unmodelled uncertainty of process model which is induced by the severe maneuvers of vehicle [8]. In a word, the uncertainty of process model is considered as ignorable in our previous works, which however is not the case for GNSS/INS of land vehicle, especially when only finite sigma points are involved in model prediction.

It is notable that the integrals involved in the moment calculation cannot be computed exactly by propagating finite samples through system function or measurement function. As a non-parameter modeling method, the Gaussian process (GP) represents posterior distributions over functions based on training data [24], which can calibrate the stochastic uncertainty of applying finite samples for moment matching. In order to enhance the robustness of KFs, GP models have been introduced to account for the system model and measurement model, which achieves better results than its parametric counterparts when given enough training data [25]. In the application of GNSS/INS, GP has also been used to enhance central difference KF, which however needs the ground truth to identify the residue between approximated model and reference model [26]. Recently, a quadrature rule named Gaussian process quadrature (GPQ) is proposed to further account for the uncertainty consisted in numerically computed moments, base on which a new quadrature KF is derived without a model identification step [27]. However, the GPQ-based KF may still suffer from non-Gaussian measurement noise, and the fixed selection of kernel parameters for GP measurement model approximation is invalid due to the changing sensor environment, which is not the case for process model. In a word, the GP-based model prediction can improve CKF by calibrating the uncertainty consisted in the moments approximation of system function.

In our previous work, we have shown that RCKF can retain some non-Gaussian and higher order information of approximated posterior PDF [21], [23]. Unlike the above-mentioned works, the aim of this paper is to develop a GPQ-enhanced RCKF for GNSS/INS, which can further improve the attitude of GNSS/INS by considering the uncertainties consisted in process model. The novelty of this work is that not only the uncertainty consisted in moments computation of prior PDF is considered but also the efficiency of GP model prediction is improved by applying the posterior PDF approximated by the NSUF-based KF update.

The structure of this paper is arranged as follows. Section II reviews the filter model of GNSS/INS and the NSUF-based CKF briefly. In Section III, the GP enhanced robust CKF is given after discussing GP-based uncertainty calibration in the context of sigma points-based moments prediction. Numerical simulation based on field test data is reported in Section IV. Finally, Section V concludes this paper.

II. MODEL AND PROBLEM FORMULATION

A. FILTER MODEL OF GNSS/INS

The navigation frame of this paper is earth-centered earth-fixed frame (e-frame), and the error state model of INS is selected as the system function of GNSS/INS. The observation of GNSS is resolved in e-frame, and the IMU is fixed in the body frame (b-frame) of vehicle which measures the angular motion and specific force of vehicle with respect to the geocentric inertial frame (i-frame). The state of GNSS/INS is $\mathbf{x} = \left(\begin{array}{cccc}\delta\boldsymbol{\psi} & \delta\mathbf{v} & \delta\mathbf{p} & \mathbf{b}_a \ \mathbf{b}_g\end{array}\right)^T$, where $\delta\boldsymbol{\psi}$ indicates the attitude error resolving in e-frame, $\delta\mathbf{v}$ and $\delta\mathbf{p}$ represents the velocity and position error respectively, $\mathbf{b}_a$ and $\mathbf{b}_g$ are the biases of accelerometers and gyroscopes. In the following discussion, we omit the time index t for brevity and clarity reasons, e.g., $\delta\dot{\boldsymbol{\psi}}(t)$ will be denoted by $\delta\dot{\boldsymbol{\psi}}$. The attitude error equation of INS resolving in e-frame is given by

$$\delta\dot{\boldsymbol{\psi}} = -\boldsymbol{\omega}_{ie}^{e} \otimes \delta\boldsymbol{\psi} + \mathbf{C}_b^e \mathbf{b}_g \tag{1}$$

where $\boldsymbol{\omega}_{ie}^{e}$ is the earth angular rate with respect to i-frame, $\mathbf{C}_b^e$ is the rotation matrix from b-frame to e-frame, and $\otimes$ represents the skew symmetric matrix. The update of attitude in e-frame refers to the update of $\mathbf{C}_b^e$ based on $\boldsymbol{\omega}_{ib}^{b}$, and it can be written as

$$\mathbf{C}_b^e(+) \approx \mathbf{C}_b^e(-)\left(\mathbf{I}_3 + \boldsymbol{\Omega}_{ib}^{b}\tau_i\right) - \boldsymbol{\Omega}_{ie}^{e}\mathbf{C}_b^e(-)\tau_i \tag{2}$$

where $\boldsymbol{\Omega}_{ib}^{b} = \boldsymbol{\omega}_{ib}^{b}\otimes$, $\boldsymbol{\Omega}_{ie}^{e} = \boldsymbol{\omega}_{ie}^{e}\otimes$, $\mathbf{C}_b^e(-)$ is the transform matrix of last time instant, $\mathbf{C}_b^e(+)$ is the updated matrix after applying $\boldsymbol{\omega}_{ib}^{b}$, $\mathbf{I}_3$ is the identity matrix of 3 dimension, and τ_i is the integration interval of angular-rate measurement. The "$\approx$" indicates that we consider the $\boldsymbol{\omega}_{ib}^{b}$ over τ_i is constant, and the exponents term contained in $\mathbf{C}_b^e$ update is approximated by its first order Taylor series expansion. The error equation of velocity and position are given by

$$\begin{aligned}\delta\dot{\mathbf{v}}_{eb}^{e} = &-\left(\mathbf{C}_b^e\mathbf{f}_{ib}^{b}\right)\otimes\delta\boldsymbol{\psi} - 2\boldsymbol{\omega}_{ie}^{e}\otimes\delta\mathbf{v}_{eb}^{e} \\ &+\frac{2g_0}{r_{eS}^{e}}\frac{\mathbf{p}_{eb}^{e}}{\left|\mathbf{p}_{eb}^{e}\right|^2}\left(\mathbf{p}_{eb}^{e}\right)^T\delta\mathbf{p}_{eb}^{e} + \mathbf{C}_b^e\mathbf{b}_a\end{aligned} \tag{3}$$

$$\delta\dot{\mathbf{p}}_{eb}^{e} = \delta\mathbf{v}_{eb}^{e} \tag{4}$$

where g_0 is the acceleration due to local gravity, r_{eS}^{e} is the geocentric radius at the earth surface. The update of $\mathbf{v}_{eb}^{e}$ is written as

$$\mathbf{v}_{eb}^{e}(+) \approx \mathbf{v}_{eb}^{e}(-) + \left(\mathbf{f}_{ib}^{e} + \mathbf{g}_b^e\left(\mathbf{p}_{eb}^{e}(-)\right) - 2\Omega_{ie}^{e}\mathbf{v}_{eb}^{e}(-)\right)\tau_i \tag{5}$$

where $\mathbf{f}_{ib}^{e} = \frac{1}{2}\left(C_b^e(-) + C_b^e(+)\right)\mathbf{f}_{ib}^{b}$, $\mathbf{g}_b^e\left(\mathbf{p}_{eb}^{e}(-)\right)$ is the local gravity resolving in e-frame, $\mathbf{v}_{eb}^{e}(-)$ and $\mathbf{v}_{eb}^{e}(+)$ are the velocity before and after the application of $\mathbf{f}_{ib}^{b}$, $\mathbf{p}_{eb}^{e}(-)$ is position of last time instant, and the "$\approx$" indicates that the variation of Coriolis term is neglected in the integration interval. The update of position $\mathbf{p}_{eb}^{e}$ can be written as

$$\begin{aligned}\mathbf{p}_{eb}^{e}(+) \approx &\ \mathbf{p}_{eb}^{e}(-) + \mathbf{v}_{eb}^{e}(-)\tau_i \\ &+\left(\mathbf{f}_{ib}^{e} + \mathbf{g}_b^e\left(\mathbf{p}_{eb}^{e}(-)\right) - 2\Omega_{ie}^{e}\mathbf{v}_{eb}^{e}(-)\right)\frac{\tau_i^2}{2}\end{aligned} \tag{6}$$

where the "$\approx$" indicates the assumption of velocity varies linearly can only give an approximation to the true value of position. The error equations of accelerometers and gyroscopes are given by

$$\dot{\mathbf{b}}_a = 0 \tag{7}$$

$$\dot{\mathbf{b}}_g = 0 \tag{8}$$

By combining (1), (3), (4), (6) and (7), and discretizing them we can get the system model of GNSS/INS. By using (2), (5), (6) to update the navigation parameters of INS and taking the position difference and velocity difference between GNSS and INS output as the measurement, we can formulate the filter model of GNSS/INS. More details on the filter model of GNSS/INS can refer to [28].

B. REVIEW OF NSUF-BASED CKF

In order to facilitate the following discussion, the discrete-time filter model of GNSS/INS are given by

$$\mathbf{x}_k = f(\mathbf{x}_{k-1}) + \mathbf{w}_{k-1} \tag{9}$$

$$\mathbf{z}_k = h(\mathbf{x}_k) + \boldsymbol{\nu}_k \tag{10}$$

where $\mathbf{x}_k \in \Re^n$, $\mathbf{w}_{k-1} \in \Re^n$ are the state and process noise vectors of system model, and $\mathbf{z}_k \in \Re^p$, $\boldsymbol{\nu}_k \in \Re^p$ are the observations and noise of measurement model. The system function satisfies $f : \Re^n \to \Re^n$, measurement function satisfies $h : \Re^n \to \Re^p$, and $\mathbf{x}_0$, $\mathbf{w}_{k-1}$ and $\boldsymbol{\nu}_k$ are mutually independent. Under Gaussian assumption, the prior PDF and posterior PDF of state can be written as $p(\mathbf{x}_k|\mathbf{Z}_{k-1}) = N\left(\mathbf{x}_k; \hat{\mathbf{x}}_{k|k-1}, \mathbf{P}_{k|k-1}\right)$ and $p(\mathbf{x}_k|\mathbf{Z}_k) = N\left(\mathbf{x}_k; \hat{\mathbf{x}}_{k|k}, \mathbf{P}_{k|k}\right)$, where $\mathbf{Z}_k = \mathbf{z}_{1:k}$ is the measurement from time 1 until time k, and $N(\mathbf{x}; \bar{\mathbf{x}}, \mathbf{P})$ denotes a Gaussian distribution of variable $\mathbf{x}$ with mean $\bar{\mathbf{x}}$ and variance $\mathbf{P}$. The sigma points of CKF for prior PDF approximation are generated by

$$\mathbf{x}_{k-1|k-1}^{i} = \begin{cases}\hat{\mathbf{x}}_{k-1|k-1} + \left(\sqrt{n\mathbf{P}_{k-1|k-1}}\right)_i & i = 1, \cdots, n \\ \hat{\mathbf{x}}_{k-1|k-1} - \left(\sqrt{n\mathbf{P}_{k-1|k-1}}\right)_{i-n} & i = n+1, \cdots, 2n\end{cases} \tag{11}$$

where $\left(\sqrt{n\mathbf{P}_{k-1|k-1}}\right)_i = \mathbf{e}_i\sqrt{n\mathbf{P}_{k-1|k-1}}$, and $\mathbf{e}_i \in \Re^n$ is the i-th elementary column vector. Similarly, for the likelihood function approximation, the sigma points are updated by

$$\mathbf{x}_{k|k-1}^{i} = \begin{cases}\hat{\mathbf{x}}_{k|k-1} + \left(\sqrt{n\mathbf{P}_{k|k-1}}\right)_i & i = 1, \cdots, n \\ \hat{\mathbf{x}}_{k|k-1} - \left(\sqrt{n\mathbf{P}_{k|k-1}}\right)_{i-n} & i = n+1, \cdots, 2n\end{cases} \tag{12}$$

Noting in (11) and (12), the sigma points used in function value evaluation only contain the moments of a Gaussian distribution with prescribed accuracy. The function values based on finite sigma points, e.g., $f\left(\mathbf{x}_{k-1|k-1}^{i}\right)$ and $h\left(\mathbf{x}_{k|k-1}^{i}\right)$, are dropped after calculating the moments. A NSUF is developed in [21], where the new sigma points for next filtering period is updated by formulating a transform matrix $\boldsymbol{\gamma}_k$, which is given by

$$\boldsymbol{\gamma}_k = \mathbf{L}_k^{+}\boldsymbol{\Xi}^T\left(\mathbf{L}_k^{-}\right)^{-1} \tag{13}$$

Algorithm 1 RCKF

Require: $\hat{\mathbf{x}}_{k-1|k-1}$, $\mathbf{P}_{k-1|k-1}$, $\tilde{\mathbf{x}}^{+}_{k-1|k-1}$

Model-based PDFs prediction

for $i = 1, \cdots, N$ do

$$\mathbf{X}^{+}_{i,k-1|k-1} = \hat{\mathbf{x}}_{k-1|k-1} + \tilde{\mathbf{X}}^{+}_{i,k-1|k-1}, \quad \boldsymbol{\omega}^{i}_{k} = 1/N$$

end for

$$\mathbf{X}^{-}_{i,k|k-1} = \mathrm{f}\left(\mathbf{X}^{+}_{i,k-1|k-1}\right), \ \hat{\mathbf{x}}_{k|k-1} = \sum_{i=1}^{N} \boldsymbol{\omega}^{i}_{k} \mathbf{X}^{-}_{i,k|k-1}$$

$$\mathbf{P}_{k|k-1} = \sum_{i=1}^{m} \boldsymbol{\omega}^{i}_{k} \mathbf{X}^{-}_{i,k,k-1} \left(\mathbf{X}^{-}_{i,k|k-1}\right)^{T} - \hat{\mathbf{x}}_{k|k-1}\hat{\mathbf{x}}^{T}_{k|k-1} + \mathbf{Q}_{k-1}$$

$$\hat{\mathbf{z}}_{k|k-1} = \sum_{i=1}^{N} \boldsymbol{\omega}^{i}_{k} h\left(\mathbf{X}^{-}_{i,k|k-1}\right) \tag{14}$$

$$\mathbf{P}^{zz}_{k|k-1} = \sum_{i=1}^{m} \boldsymbol{\omega}^{i}_{k} \mathrm{h}\left(\mathbf{X}^{-}_{i,k|k-1}\right) \left(\mathrm{h}\left(\mathbf{X}^{-}_{i,k|k-1}\right)\right)^{T} - \hat{\mathbf{z}}_{k|k-1}\hat{\mathbf{z}}^{T}_{k|k-1} + \mathbf{R}_{k} \tag{15}$$

$$\mathbf{P}^{\mathrm{e}}_{k|k-1} = \sum_{i=1}^{N} \boldsymbol{\omega}^{i}_{k} \mathbf{X}^{-}_{i,k|k-1} \left(\mathrm{h}\left(\mathbf{X}^{-}_{i,k|k-1}\right)\right)^{T} - \hat{\mathbf{x}}_{k|k-1}\hat{\mathbf{z}}^{T}_{k|k-1} \tag{16}$$

Update posterior moments

$\mathbf{z}_{k-1} \leftarrow \mathbf{z}_{k}$ ▷ Receive new observations

$$\mathbf{K}_{k} = \mathbf{P}^{xz}_{k|k-1}\left(\mathbf{P}^{zz}_{k|k-1}\right)^{-1}$$

$$\hat{\mathbf{x}}_{k|k} = \hat{\mathbf{x}}_{k|k-1} + \mathbf{K}_{k}\left(\mathbf{z}_{k} - \hat{\mathbf{z}}_{k|k-1}\right) \tag{17}$$

$$\mathbf{P}_{k|k} = \mathbf{P}_{k|k-1} - \mathbf{K}_{k}\mathbf{P}^{zz}_{k|k-1}\mathbf{K}^{T}_{k} \tag{18}$$

Update sigma points

Update the transform matrix use (13)

for $i = 1, \cdots, N$ do

$\tilde{\mathbf{X}}^{-}_{i,k|k} = \mathbf{X}^{-}_{i,k-1} - \hat{\mathbf{x}}_{k|k-1}$ ▷ Compute function evaluation residue

$\tilde{\mathbf{X}}^{+}_{i,k|k} = \gamma_{k}\tilde{\mathbf{X}}^{-}_{t,kk-1}$

end for

where $\mathbf{P}_{k|k-1} - \Delta\mathbf{Q} = \mathbf{L}^{-}_{k}\left(\mathbf{L}^{-}_{k}\right)^{T}$, $\mathbf{P}_{k|k} - \Delta\mathbf{R} = \mathbf{L}^{+}_{k}\left(\mathbf{L}^{+}_{k}\right)^{T}$, $\boldsymbol{\Xi}\,\boldsymbol{\Xi}^{T} = \mathbf{I}$ and $\mathbf{I}$ is the identity matrix of appropriate dimension. More details on the setting of $\Delta\mathbf{Q}$ and $\Delta\mathbf{R}$ please refer to [22], [23]. Suppose the number of sigma points is $N = 2n$, and the steps of NSUF-based CKF (RCKF) are summarized in Algorithm 1.

Remark 1: Notice that, there is uncertainty in the calculation of function evaluation residue by using finite sigma points, and also $\boldsymbol{\gamma}_{k}$ approximates to $\mathbf{0}$ when the filter becomes stable, which is an expected phenomenon for the sigma points error reduction. However, in order to ensure the filter stable it is better to add positive defined matrix to $\mathbf{P}_{k|k}$[29]. If the process uncertainties including the unmodelled model error and function evaluation error are taken into consideration in the calculation of $\boldsymbol{\gamma}_{k}$, the enlarged $\mathbf{P}_{k|k-1}$ will result in a further reduction of $\boldsymbol{\gamma}_{k}$.

Remark 2: Because the points away from the central point would lead to performance degradation in moments approximation, the sigma points generated by (11) are less efficient for high-dimensional filtering problem. What is more, the measurement model of loosely coupled GNSS/INS is linear, and R_{k} can be fine-tuned by evaluating the filter performance or using VB-based noise estimation algorithm. Consequently, we focus on the calibration of function prediction error of system model only, which has a significant effect on the attitude estimation of GNSS/INS.

III. UNCERTAINTY CALIBRATION OF SIGMA POINTS TRANSFORM

A. GAUSSIAN PROCESS QUADRATURE

Following the definition and notation in [25], we briefly review GP in the context of sigma points-based moments prediction. Let the system function f(x) distributed according to a GP satisfy GP $\left(M\left(\mathbf{X}\right), k\left(\mathbf{x}, \mathbf{x}'\right)\right)$, and the GP can be uniquely determined by its mean function m(x) and covariance function $k\left(\mathbf{x}, \mathbf{x}'\right)$. In this paper, we select squared exponential (SE) kernel as the covariance function, and the mean function is set as 0 without loss of generality. The SE kernel is given by

$$k\left(\mathbf{x}, \mathbf{x}'\right) = \alpha^{2} \exp\left(-\frac{1}{2}\left(\mathbf{x} - \mathbf{x}'\right)^{T} \Lambda \left(\mathbf{x} - \mathbf{x}'\right)\right) \tag{19}$$

where Λ are the length-scales of SE kernel and α^{2} is the variance of latent function f(x). Suppose the data $D = \{(\mathbf{x}_{i}, \mathrm{f}(\mathbf{x}_{i}))\}_{i=1}^{N}$ have been generated according to (9), where the training input $\mathbf{x}_{i} = \mathbf{x}^{i}_{k-1|k-1}$ and $\mathrm{f}(\mathbf{x}_{i})$ is the function evaluation value using $\mathbf{x}^{i}_{k-1|k-1}$, i.e., the training targets $\mathbf{y} = \left[\mathrm{f}\left(\mathbf{x}^{1}_{k-1|k-1}\right) \cdots \mathrm{f}\left(\mathbf{x}^{N}_{k-1|k-1}\right)\right]^{T}$. Then the predictive mean and variance of GP posterior $p(f \mid D)$ are given by

$$m_{\mathrm{f}}(\mathbf{x}) = E_{\mathrm{f}}[\mathrm{f}(\mathbf{x}) \mid D] = \mathrm{k}^{T}(\mathbf{x})\,\mathbf{K}^{-1}\mathbf{y} \tag{20}$$

$$\sigma^{2}_{\mathrm{f}}(\mathbf{x}) = \mathrm{V}_{\mathrm{f}}[\mathrm{f}(\mathbf{x}) \mid D] = k(\mathbf{x}, \mathbf{x}) - \mathbf{k}^{T}(\mathbf{x})\,\mathbf{K}^{-1}\mathbf{k}(\mathbf{x}) \tag{21}$$

where E[·] and V[·] denote the expectation and variance operator, $[\mathrm{k}(\mathbf{x})]_{i} = k(\mathbf{x}, \mathbf{x}_{i})$ is the i-th element of k(**x**), the element of **K** at position (i, j) is denoted as $[\mathbf{K}]_{ij} = k(\mathbf{x}_{i}, \mathbf{x}_{j}) = \mathrm{C_f}[\mathrm{f}(\mathbf{x}_{i}), \mathrm{f}(\mathbf{x}_{j})]$, and C[·] denotes the covariance operator. Because both of the uncertainty in $\mathbf{x}_{i}$ and f(·) are considered in GP, the a-th dimension of the prediction mean can be written as

$$\left(\hat{\mathbf{x}}_{k|k-1}\right)_{a} = \int m_{f_{a}}(\mathbf{x}_{k-1})\, p\left(\mathbf{x}_{k-1} \mid \mathbf{Z}_{k-1}\right) d\mathbf{x}_{k-1} = \mathbf{y}^{T}_{a}\left(\mathbf{K} + \sigma^{2}_{\mathbf{w}_{a}}\right)^{-1}\mathbf{q}^{\mathbf{x}}_{a} \tag{22}$$

where $\mathbf{y}_a$ is the a-th training target, $\sigma^2_{\mathbf{w}_a}$ is the learned system noise variance, $a = 1, \cdots, n$ and $q^{\mathbf{x}}_a$ is defined as

$$\begin{aligned}\mathbf{q}^{\mathbf{x}}_{a_i} = \alpha^2_{f_a} &\left|\mathbf{P}_{k-1|k-1}\Lambda_a^{-1} + \mathbf{I}\right|^{-\frac{1}{2}} \\ &\times \exp\left(-\frac{1}{2}\left(\mathbf{x}_i - \hat{\mathbf{x}}_{k-1|k-1}\right)^T \left(\mathbf{P}_{k-1|k-1} + \Lambda_a\right)^{-1}\right. \\ &\left.\times \left(\mathbf{x}_i - \hat{\mathbf{x}}_{k-1|k-1}\right)\right) \end{aligned} \tag{23}$$

where α_{f_a} and Λ_a are the hyper-parameters learned by using sigma points corresponding to the a-th target of GP model. Let $b = 1, \cdots, n$, and the entries of prediction covariance are given by

$$\begin{aligned}\left(\mathbf{P}_{k|k-1}\right)_{ab} = E_{\mathbf{x}_{k-1}}&\left[C_{\mathrm{f}}\left[\mathrm{f}_a\left(\mathbf{x}_{k-1}\right), \mathrm{f}_b\left(\mathbf{x}_{k-1}\right)\middle|\mathbf{x}_{k-1}\right]\middle|\mathbf{Z}_{k-1}\right] \\ &+C_{\mathbf{x}_{k-1}}\left[E_{\mathrm{f}_a}\left[f_a\left(\mathbf{x}_{k-1}\right)\middle|\mathbf{x}_{k-1}\right],\right. \\ &\left.E_{\mathrm{f}_b}\left[\mathrm{f}_b\left(\mathbf{x}_{k-1}\right)\middle|\mathbf{x}_{k-1}\right]\middle|\mathbf{Z}_{k-1}\right] \end{aligned} \tag{24}$$

Inserting (20) and (22) into the second term of (24), we get

$$\begin{aligned}&C_{\mathbf{x}_{k-1}}\left[m_{\mathrm{f}_a}\left(\mathbf{x}_{k-1}\right), m_{\mathrm{f}_b}\left(\mathbf{x}_{k-1}\right)\middle|\mathbf{Z}_{k-1}\right] \\ &\quad = \left(\beta^x_a\right)^T \mathbf{Q}\left(\beta^x_b\right) - \left(\hat{\mathbf{x}}_{k|k-1}\right)_a \left(\hat{\mathbf{x}}_{k|k-1}\right)_b \end{aligned} \tag{25}$$

By defining $\varsigma_i = \mathbf{x}_i - \hat{\mathbf{x}}_{k-1|k-1}$, $z_{i,j} = \Lambda_a^{-1}\varsigma_i + \Lambda_b^{-1}\varsigma_j$ and $\mathbf{R} = \mathbf{P}_{k-1|k-1}\left(\Lambda_a^{-1} + \Lambda_b^{-1}\right) + \mathbf{I}$, the entries of $\mathbf{Q}$ can be written as

$$\begin{aligned}\mathbf{Q}_{ij} &= k_{f_a}\left(\mathbf{x}_i, \hat{\mathbf{x}}_{k-1|k-1}\right) k_{f_b}\left(\mathbf{x}_j, \hat{\mathbf{x}}_{k-1|k-1}\right) \\ &\quad\times \exp\left(\frac{1}{2}\mathbf{z}_{ij}^T\mathbf{R}^{-1}\mathbf{P}_{k-1|k-1}\mathbf{z}_{ij}\right)/\sqrt{|\mathbf{R}|} \\ &= \left[\log\left(\alpha^2_{f_a}\right) + \log\left(\alpha^2_{f_b}\right) - \frac{1}{2}\left(\varsigma_i^T\Lambda_a^{-1}\varsigma_i + \varsigma_j^T\Lambda_b^{-1}\varsigma_j\right.\right. \\ &\quad\left.\left. - \mathbf{z}_{ij}^T\mathbf{R}^{-1}\mathbf{P}_{k-1|k-1}\mathbf{z}_{ij}\right)\right]/\sqrt{|\mathbf{R}|} \end{aligned} \tag{26}$$

Let tr$(\cdot)$ denote the trace operator, and the first term of (24) is non-zero only when $a = b$, where the entries of expected covariance is given as

$$\begin{aligned}&\mathrm{E}_{\mathbf{x}_{k-1}}\left[C_{\mathrm{f}}\left[\mathrm{f}_a\left(\mathbf{x}_{k-1}\right), \mathrm{f}_b\left(\mathbf{x}_{k-1}\right)\middle|\mathbf{x}_{k-1}\right]\middle|\mathbf{Z}_{k-1}\right] \\ &\quad = \alpha^2_{\mathrm{f}_a} - \mathrm{tr}\left(\left(\mathbf{K} + \sigma^2_{\mathbf{w}_a}\right)^{-1}\mathbf{Q}\right) + \sigma^2_{\mathbf{w}_a} \end{aligned} \tag{27}$$

Then the prediction covariance matrix in (24) can be obtained by (25) when $a \neq b$ or by adding (27) to (25) in case $a = b$.

B. DISCUSSION ON GPQ ENHANCED NSUF

By combining the GPQ-based model prediction and the measurement update of RCKF, we develop an enhanced RCKF, named as GP-RCKF in this paper. In case only position and velocity are used as the observations for GNSS/INS, the correction information of attitude appears in the prediction stage of KF and we only modify the state prediction of RCKF to reducing the complexity of GP-RCKF. The flowchart of GP-RCKF is shown in Fig. 1.

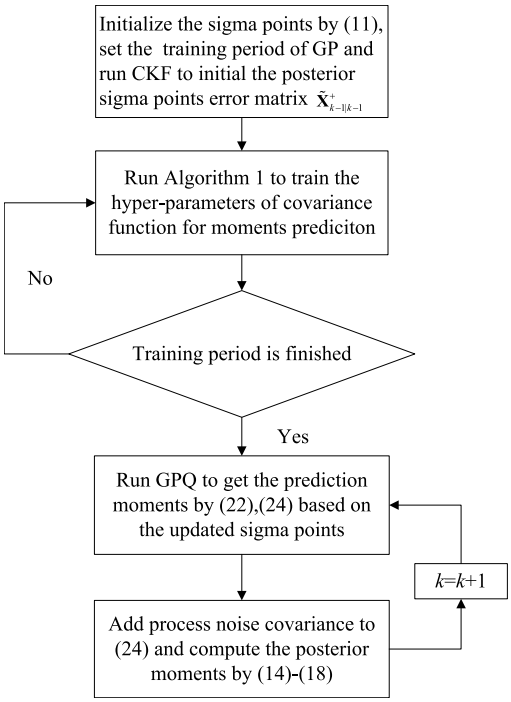

FIGURE 1. Flowchart of GPQ enhanced RCKF.

Define $\Phi_{k|k-1} = \partial \mathrm{f}\left(\mathbf{x}_{k-1}\right)/\partial\mathbf{x}_{k-1}$, $\mathbf{H}_k = \partial \mathrm{h}(\mathbf{x}_k)/\partial\mathbf{x}_k$, and the predicted error vectors by (9) and (10) can be formulated as

$$\begin{aligned}\tilde{\mathbf{x}}_{k|k-1} &= \left(\Phi_{k|k-1} + \mathbf{A}_k\mathbf{N}_{f,k}\Theta_{f.k}\right)\tilde{\mathbf{x}}_{k-1|k-1} \\ &\quad + \mathbf{B}_k\Delta_{Bk}\mathbf{E}_{Bk}\mathbf{x}_{k-1} + \mathbf{w}_{k-1} \end{aligned} \tag{28}$$

$$\begin{aligned}\tilde{\mathbf{z}}_{k|k-1} &= \left(\mathbf{H}_k + \mathbf{C}_k\mathbf{N}_{h,k}\Theta_{h,k}\right)\tilde{\mathbf{x}}_{k|k-1} \\ &\quad + \mathbf{D}_k\Delta_{Dk}\mathbf{E}_{Dk}\mathbf{x}_k + \boldsymbol{\nu}_k \end{aligned} \tag{29}$$

where $\mathbf{A}_k$ and $\mathbf{C}_k$ are problem dependent scaling matrices, $\tilde{\mathbf{x}}_{k|k-1} = \mathbf{x}_k - \hat{\mathbf{x}}_{k|k-1}$, $\tilde{\mathbf{z}}_{k|k-1} = \mathbf{z}_k - \hat{\mathbf{z}}_{k|k-1}$, $\tilde{\mathbf{x}}_{k-1|k-1} = \mathbf{x}_k - \hat{\mathbf{x}}_{k-1|k-1}$, $\mathbf{N}_{f,k}$ and $\mathbf{N}_{h,k}$ are unknown time-varying linearization error of f$(\cdot)$ and h$(\cdot)$, $\Theta_{f.k}$ and $\Theta_{h,k}$ provide an extra degree of freedom for filter tune. $\mathbf{B}_k\Delta_{Bk}\mathbf{E}_{Bk}\mathbf{x}_{k-1}$ and $\mathbf{D}_k\Delta_{Dk}\mathbf{E}_{Dk}\mathbf{x}_k$ denote the unmodelled uncertainties, where $\mathbf{B}_k$ and $\mathbf{D}_k$ are known scaling matrices, $\Delta_{Bk} \in \Re^{n\times n}$, $\Delta_{Dk} \in \Re^{n\times n}$ and satisfying $E[\Delta_{Bk}\Delta_{Bk}^T] \leq \mathbf{I}$, $E[\Delta_{Dk}\Delta_{Dk}^T] \leq \mathbf{I}$, $\mathbf{E}_{Bk}$ and $\mathbf{E}_{Dk}$ are known and can be set as $\mathbf{I}$ here. Then we have *Theorem 3.1* for the prior covariance and posterior covariance corresponding to (28) and (29).

Theorem 3.1: For system (9) and (10) with bounded noise and unmodelled uncertainties, the predication covariance and posterior covariance are given by

$$\begin{aligned}\mathbf{P}_{k|k-1} &= \left(\Phi_{k|k-1} + \mathbf{A}_k\mathbf{N}_{f,k}\Theta_{f.k}\right)\mathbf{P}_{k-1|k-1}\left(\Phi_{k|k-1}\right. \\ &\quad\left. + \mathbf{A}_k\mathbf{N}_{f,k}\Theta_{f.k}\right)^T + \Delta\mathbf{P}_{k|k-1} + \mathbf{Q}_{k-1} \end{aligned} \tag{30}$$

$$\begin{aligned}\mathbf{P}_{k|k} &= \left[\mathbf{I} - \mathbf{K}_k\left(\mathbf{H}_{k|k-1} + \mathbf{C}_k\mathbf{N}_{h,k}\Theta_{h,k}\right)\right] \\ &\quad\times\mathbf{P}_{k|k-1}\left[\mathbf{I} - \mathbf{K}_k\left(\mathbf{H}_{k|k-1} + \mathbf{C}_k\mathbf{N}_{h,k}\Theta_{h,k}\right)\right]^T \\ &\quad + \mathbf{K}_k\left(\Delta\mathbf{P}_k + \mathbf{R}_k\right)\mathbf{K}_k^T \end{aligned} \tag{31}$$

where

$$\Delta\mathbf{P}_{k|k-1} = \mathbf{B}_k \mathrm{E}\left[\Delta_{Bk}\mathbf{x}_{k-1}\mathbf{x}_{k-1}^T\Delta_{Bk}^T\right]\mathbf{B}_k^T$$
$$\Delta\mathbf{P}_k = \mathbf{D}_k \mathrm{E}\left[\Delta_{Dk}\mathbf{x}_{k-1}\mathbf{x}_{k-1}^T\Delta_{Dk}^T\right]\mathbf{D}_k^T$$

and both (30) and (31) are bounded.

Proof: See the proof given in Appendix A of [21].

Remark 3: Notice that, the unmodelled uncertainties terms $\mathbf{B}_k\Delta_{Bk}\mathbf{E}_{Bk}\mathbf{x}_{k-1}$, $\mathbf{D}_k\Delta_{Dk}\mathbf{E}_{Dk}\mathbf{x}_k$ are linear function of underlying state, and the matrices $\mathbf{B}_k$ and $\mathbf{D}_k$ are considered as known but hard to tune in practical. In the GPQ-based model prediction framework, the effect of these terms can be compensated by using the learned instantiated function values partly, which does not need parameter tune and in turn provides better result compared with normal sigma-point Kalman filter without fixing these terms.

Remark 4: Because the measurement model of loosely coupled GNSS/INS is linear, and the time-varying measurement noise can be online estimated, we do not apply GPQ for measurement function transform. What is more, the hyper-parameters for GP measurement model after the training period are hardly suitable for model prediction because of the changing sensor environment. Therefore, in order to enhance the attitude estimation of GNSS/INS without increasing the complexity obviously, only the uncertainty of system function transform is handled by GPQ in our algorithm.

IV. FIELD TESTS

The error of navigation state is selected as the state to be estimated, and a closed-form filter loop is used to update the state recursively. The field test setups are shown in Fig. 2, where a NovAtel SPAN system is employed to record the sensors' data. The specific characteristics of the involved IMU are listed in Table 1. The raw data sets of GNSS receiver and IMU output are then post-processed by the Waypoint Inertial Explorer and the proposed algorithms, respectively, where the former is taken as the ground truth. By logging the raw data records with GNSS 1PPS, it is easily to integrate the output data of different frequencies in post-processing way. The update frequencies of GNSS, IMU and the post-processing software are 5Hz, 200Hz and 100Hz, respectively.

The trajectory of the field test is shown in Fig. 3, where a signal outage (less than 5 s) is flagged by a purple circle. In our simulation, all the filters use the same configuration parameters including $\mathbf{P}_{0|0}$, $\mathbf{Q}_{k-1}$ and $\mathbf{R}_k$ making the comparison among the filters fair. What is more, we utilize the VB-based measurement noise estimation algorithm proposed in [18] and applied in [20] to compare the VB-based adaptive CKF, named as VB-CKF, with our proposed algorithm. Because the training stage is time-consuming, we use the sigma points and the function values from 30th to 60th epoch for hyper-parameters learning, and then the learned hyper-parameters are applied for system function transform.

The output trajectories of different CKFs are shown in Fig. 4 and Fig. 5, where the result of different filters under signal outage and frequent angular motion are given. It is

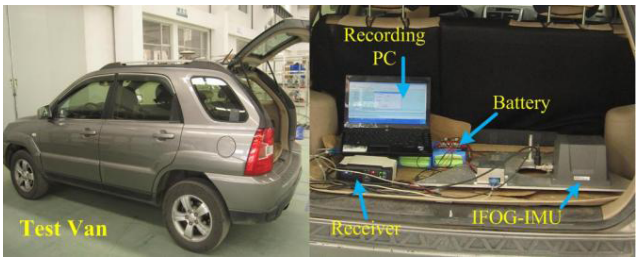

FIGURE 2. Field test setups.

TABLE 1. Specifications of sensors in IMU.

Sensor	Characteristic	Value
Gyroscope	Rate bias offset	1 deg/hr
	Rate scale factor	100 ppm
	Angular random walk	0.071 deg/rt-hr
Accelerometer	Bias	0.3 mg
	Scale factor	300 ppm
	Linerarity	150 ppm

FIGURE 3. Trajectory of field test, the purple circle marks a signal outage less than 5 s.

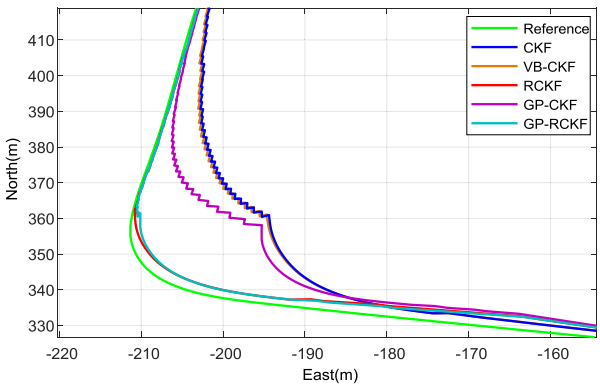

FIGURE 4. Position output of different filters under GNSS outage.

notable that GP-CKF outperforms CKF and VB-CKF when GNSS outage appears which indicates that GPQ enhanced the estimation of IMU biases when no observations are available. Notice that, when the vehicle runs in frequent angular motion there are obvious steady-state errors for CKF and VB-CKF, which demonstrates that the unmodelled

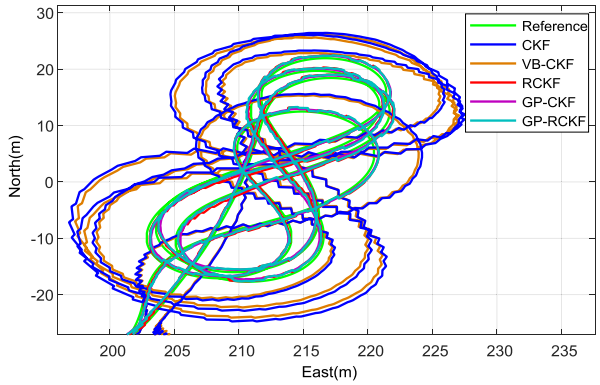

FIGURE 5. Position output of different filters under frequent angular motion.

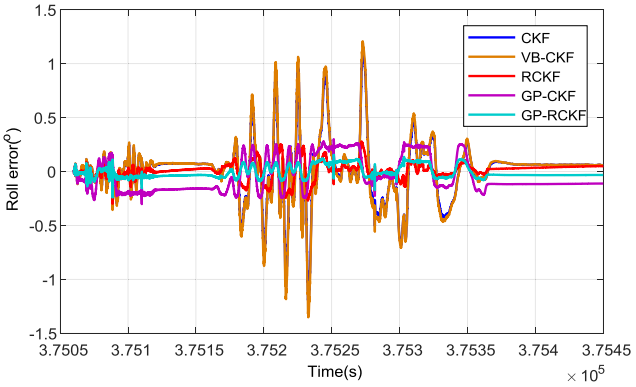

FIGURE 6. Roll error of different filters.

uncertainties in system model would degrade the performance of CKF even if the observations are available. However, because GP-CKF utilizes the traditional sigma points update framework, the accuracy of posterior covariance still has a great effect on its position result in case a signal outage present. By employing the NSUF, both RCKF and GP-RCKF show better trajectory tracking result than the CKFs utilizing sigma points generated by (11) and (12), which indicates the efficiency of sigma points spanned by the posterior sigma points error matrix.

Unlike position which is of strong observability in GNSS/INS filtering, the attitude is of weak observability and the heading would diverge in case the vehicle goes along a straight line. The roll and pitch result of GNSS/INS are shown in Fig. 6 and Fig. 7, respectively, where both GP-CKF and GP-RCKF perform better than their non-GPQ enhanced counterparts. What is more, the result of GP-CKF is worse than NSUF-based CKFs, i.e., RCKF and GP-RCKF, and more detailed results are listed in Table 2. In Table 2, the RMSE of attitude and the average RMSE of position are given, and the latter is defined by

$$AP = \sqrt{\frac{1}{2}\left(E_{RMSE}^2 + N_{RMSE}^2\right)}, \tag{32}$$

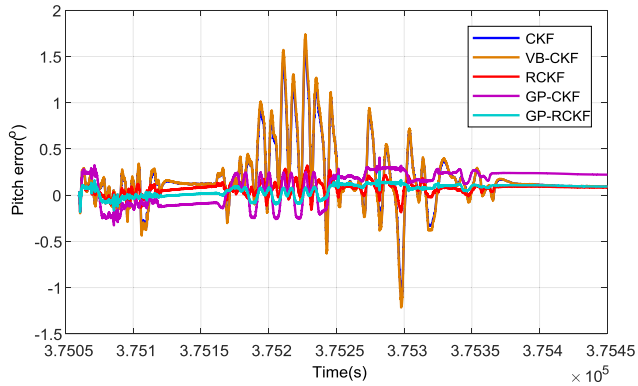

FIGURE 7. Pitch error of different filters.

TABLE 2. RMSE of vehicle attitude and average RMSE of position for different filters.

Algorithm	Heading(°)	Roll(°)	Pitch(°)	*AP*(m)
CKF	2.41	0.27	0.37	6.61
VB-CKF	2.92	0.28	0.38	**6.58**
RCKF	0.86	0.08	0.09	6.48
GP-CKF	0.35	0.16	0.20	**6.63**
GP-RCKF	**0.34**	**0.05**	**0.08**	6.49

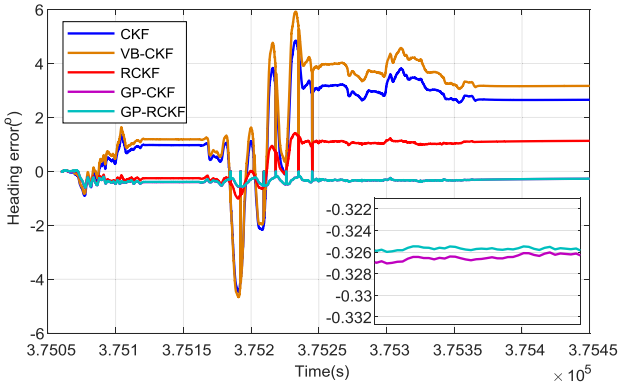

FIGURE 8. Heading error of different filters.

where E_{RMSE}, N_{RMSE} represent the RMSE of position in east and north direction. Result of heading is shown in Fig. 8, and noting that by employing GPQ to enhance the prediction stage based on (9), the heading is improved obviously. The VB-CKF does not achieve better results than CKF in terms of attitude, but achieves a slight better result in terms of position, which indicates the time-varying measurement noise does affect the performance of position.

Noting Table 2, compared with CKF, GP-CKF does not perform better in terms of *AP*, and on the contrary it degrades the position. Furthermore GP-RCKF reduces the error of attitude obviously but shows similar result when compared with RCKF in terms of *AP*. Because the correction information of attitude error mainly comes from the off-diagonal

elements of prediction covariance, the improvement of attitude demonstrates the enhancement of prediction covariance. The reason for position degradation may come from the unmodelled measurement uncertainties, e.g., the time-varying measurement noise, which underestimates the posterior covariance making the Kalman gain decreases quickly. As the learning of the hyper-parameters can be done off-line, we can further improve the training stage by using other more accurate sigma points, such as generated by smoother-based posterior PDF. What is more, increasing the training period would surely improve the quality of learned hyper-parameters and thus the prediction covariance.

V. CONCLUSION

In order to improve the prediction stage of RCKF which is very important for attitude estimation of GNSS/INS, a GPQ-based novel sigma-point update framework (NSUF) is proposed in the context of sigma points-based moments matching. Based on the GPQ-based NSUF, an improved robust CKF, named as GP-RCKF, is derived by the authors to process the uncertainty existing in system function transform. The GP-RCKF is verified by field test data, and simulation results demonstrate that GP-RCKF improves the heading by 60.5% compared with RCKF without degrading the position result obviously.

It is notable that we only train the hyper-parameters of GP system prediction model when the vehicle goes along straight line at almost constant velocity, more works should be done to train the hyper-parameters according to the observability analysis of GNSS/INS [30]. Further study will also be focused on more widely application of non-parameter transform for nonlinear filters design, e.g., non-parameter form of (13) for sigma points error matrix transform.

ACKNOWLEDGMENT

B. Cui would like to thank Dr. S. Wang, Dr. B. Shi from Shandong University of Science and Technology (China) for their help in collecting field test data.

REFERENCES

[1] G. Falco, M. Nicola, and M. Pini, "Positioning based on tightly coupled multiple sensors: A practical implementation and experimental assessment," *IEEE Access*, vol. 6, pp. 13101–13116, 2018.
[2] S. Julier, J. Uhlmann, and H. Durrant-Whyte, "A new method for the nonlinear transformation of means and covariances in filters and estimators," *IEEE Trans. Autom. Control*, vol. 45, no. 3, pp. 477–482, Mar. 2000.
[3] J. Dunik, M. Simandl, and O. Straka, "Unscented Kalman filter: Aspects and adaptive setting of scaling parameter," *IEEE Trans. Autom. Control*, vol. 57, no. 9, pp. 2411–2416, Sep. 2012.
[4] I. Arasaratnam and S. Haykin, "Cubature Kalman filters," *IEEE Trans. Autom. Control*, vol. 54, no. 6, pp. 1254–1269, Jun. 2009.
[5] B. Jia, M. Xin, and Y. Cheng, "High-degree cubature Kalman filter," *Automatica*, vol. 49, no. 2, pp. 510–518, Feb. 2013.
[6] B. Jia, M. Xin, and Y. Cheng, "Sparse-grid quadrature nonlinear filtering," *Automatica*, vol. 48, no. 2, pp. 327–341, Feb. 2012.
[7] B. Chen, X. Liu, H. Zhao, and J. C. Principe, "Maximum correntropy Kalman filter," *Automatica*, vol. 76, pp. 70–77, Feb. 2017.
[8] L. Chang, K. Li, and B. Hu, "Huber's M-estimation-based process uncertainty robust filter for integrated INS/GPS," *IEEE Sensors J.*, vol. 15, no. 6, pp. 3367–3374, Jun. 2015.
[9] M. S. Arulampalam, S. Maskell, N. Gordon, and T. Clapp, "A tutorial on particle filters for online nonlinear/non-Gaussian Bayesian tracking," *IEEE Trans. Signal Process.*, vol. 50, no. 2, pp. 174–188, Feb. 2002.
[10] T. Schon, F. Gustafsson, and P.-J. Nordlund, "Marginalized particle filters for mixed linear/nonlinear state-space models," *IEEE Trans. Signal Process.*, vol. 53, no. 7, pp. 2279–2289, Jul. 2005.
[11] V. Smidl and A. Quinn, "Variational Bayesian filtering," *IEEE Trans. Signal Process.*, vol. 56, no. 10, pp. 5020–5030, Oct. 2008.
[12] S. Han, D. Luo, W. Meng, and C. Li, "Antispoofing RAIM for dual-recursion particle filter of GNSS calculation," *IEEE Trans. Aerosp. Electron. Syst.*, vol. 52, no. 2, pp. 836–851, Apr. 2016.
[13] B. Cui, X. Chen, Y. Xu, H. Huang, and X. Liu, "Performance analysis of improved iterated cubature Kalman filter and its application to GNSS/INS," *ISA Trans.*, vol. 66, pp. 460–468, Jan. 2017.
[14] T. Ardeshiri, E. Ozkan, U. Orguner, and F. Gustafsson, "Approximate Bayesian smoothing with unknown process and measurement noise covariances," *IEEE Signal Process. Lett.*, vol. 22, no. 12, pp. 2450–2454, Dec. 2015.
[15] P. Dong, Z. Jing, H. Leung, and K. Shen, "Variational Bayesian adaptive cubature information filter based on wishart distribution," *IEEE Trans. Autom. Control*, vol. 62, no. 11, pp. 6051–6057, Nov. 2017.
[16] L. Luo, Y. Zhang, T. Fang, and N. Li, "A new robust Kalman filter for SINS/DVL integrated navigation system," *IEEE Access*, vol. 7, pp. 51386–51395, 2019.
[17] H. Nurminen, T. Ardeshiri, R. Piche, and F. Gustafsson, "Skew-*t* filter and smoother with improved covariance matrix approximation," *IEEE Trans. Signal Process.*, vol. 66, no. 21, pp. 5618–5633, Nov. 2018.
[18] Y. Huang, Y. Zhang, Y. Zhao, and J. A. Chambers, "A novel robust Gaussian–student's t mixture distribution based Kalman filter," *IEEE Trans. Signal Process.*, vol. 67, no. 13, pp. 3606–3620, Jul. 2019.
[19] S. Sarkka and A. Nummenmaa, "Recursive noise adaptive Kalman filtering by variational Bayesian approximations," *IEEE Trans. Autom. Control*, vol. 54, no. 3, pp. 596–600, Mar. 2009.
[20] C. Sun, Y. Zhang, G. Wang, and W. Gao, "A new variational Bayesian adaptive extended Kalman filter for cooperative navigation," *Sensors*, vol. 18, no. 8, p. 2538, Aug. 2018.
[21] B. Cui, X. Chen, and X. Tang, "Improved cubature Kalman filter for GNSS/INS based on transformation of posterior sigma-points error," *IEEE Trans. Signal Process.*, vol. 65, no. 11, pp. 2975–2987, Jun. 2017.
[22] B. Cui, X. Wei, X. Chen, J. Li, and A. Wang, "Robust cubature Kalman filter based on variational Bayesian and transformed posterior sigma points error," *ISA Trans.*, vol. 86, pp. 18–28, Mar. 2019.
[23] B. Cui, X. Wei, X. Chen, J. Li, and L. Li, "On sigma-point update of cubature Kalman filter for GNSS/INS under GNSS-challenged environment," *IEEE Trans. Veh. Technol.*, vol. 68, no. 9, pp. 8671–8682, Sep. 2019.
[24] J. Ko and D. Fox, "GP-BayesFilters: Bayesian filtering using Gaussian process prediction and observation models," *Auton Robot*, vol. 27, no. 1, pp. 75–90, Jul. 2009.
[25] M. P. Deisenroth, R. D. Turner, M. F. Huber, U. D. Hanebeck, and C. E. Rasmussen, "Robust filtering and smoothing with Gaussian processes," *IEEE Trans. Autom. Control*, vol. 57, no. 7, pp. 1865–1871, Jul. 2012.
[26] W. Ye, J. Li, J. Fang, and X. Yuan, "EGP-CDKF for performance improvement of the SINS/GNSS integrated system," *IEEE Trans. Ind. Electron.*, vol. 65, no. 4, pp. 3601–3609, Apr. 2018.
[27] J. Pruher and O. Straka, "Gaussian process quadrature moment transform," *IEEE Trans. Autom. Control*, vol. 63, no. 9, pp. 2844–2854, Sep. 2018.
[28] P. D. Groves, *Principles of GNSS, Inertial, and Multisensor Integrated Navigation Systems*, 3rd ed. Boston, MA, USA: Artech House, 2013, pp. 584–606.
[29] K. Xiong, H. Y. Zhang, and C. W. Chan, "Performance evaluation of UKF-based nonlinear filter," *Automatica*, vol. 42, no. 2, pp. 261–270, 2006.
[30] Y. Tang, Y. Wu, M. Wu, W. Wu, X. Hu, and L. Shen, "INS/GPS integration: Global observability analysis," *IEEE Trans. Veh. Technol.*, vol. 58, no. 3, pp. 1129–1142, Mar. 2009.

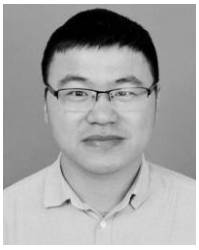

BINGBO CUI (Member, IEEE) received the B.S. and M.S. degrees in measurement, control and instrument from the Chongqing University of Technology, Chongqing, China, in 2005 and 2012, respectively, and the Ph.D. degree in precision instrument and machinery from Southeast University, Nanjing, China, in 2017. Since November 2017, he has been an Assistant Professor with the School of Agricultural Equipment Engineering, Jiangsu University, Zhenjiang, China. His research interests include inertial navigation, nonlinear filtering, integrated navigation and their application in autonomous vehicle control. He received the Excellent Doctoral Dissertation of Jiangsu Province and the National Excellent Doctoral Dissertation Award Nomination of China Instrument and Control Society, in 2019.

XINHUA WEI received the B.S. degree from the School of Mechanical and Electrical Engineering, Shandong Agricultural University (SAU), Taian, China, in 1994, the M.S. degree from the College of Engineering, China Agricultural University, Beijing, China, in 1997, and the Ph.D. degree in measurement technology and automatic equipment from Southeast University, in 2008. From March 1997 to March 2004, he was an Associate Professor with the School of Mechanical and Electrical Engineering, SAU. He joined Jiangsu University, in 2008, where he is currently a Professor. His current research interests include agricultural information intelligent perception, agricultural robot, and unmanned agricultural machinery.

XIYUAN CHEN (Senior Member, IEEE) received the B.S. degree in mechanical engineering from the Lanzhou University of Technology, Lanzhou, China, in 1990, the M.S. degree in mechanical engineering from the Hefei University of Technology, China, in 1995, and the Ph.D. degree in precision instrument and machinery from Southeast University, China, in 1998. From October 2005 to September 2006, he was a Visiting Scholar with the Department of Electronic Engineering, Politecnico di Torino, Italy. He is currently a Professor with the School of Instrument Science and Engineering, Southeast University. He has authored or coauthored more than 200 articles and 60 issued patents. His research interests include fiber optic sensors, inertial navigation, GNSS software receiver and wireless location technologies, integrated navigation, and related application.

AICHEN WANG received the B.S. degree from the College of Engineering, Huazhong Agriculture University (HZAU), Wuhan, China, in 2011, and the Ph.D. degree in agricultural engineering from Zhejiang University, in 2017. He joined Jiangsu University, in 2017, where he is currently a Research Associate. His current research interests include agricultural information intelligent perception, agricultural robot, and unmanned agricultural machinery.